Design of Natural Damping Control for Three-phase Grid-Connected Voltage Source Inverters with LCL-Filters

John Onoghenokpe Mogah

Submitted to the
Institute of Graduate Studies and Research
in partial fulfillment of the requirements for the degree of

Master of Science
in
Electrical and Electronic Engineering

Eastern Mediterranean University
July 2017
Gazimağusa, North Cyprus

Approval of the Institute of Graduate Studies and Research

Prof. Dr. Mustafa Tümer
Director

I certify that this thesis satisfies the requirements as a thesis for the degree of Master of Science in Electrical and Electronic Engineering.

Prof. Dr. Hassan Demirel
Chair, Department of Electrical and Electronic Engineering

We certify that we have read this thesis and that in our opinion it is fully adequate in scope and quality as a thesis for the degree of Master of Science in Electrical and Electronic Engineering.

Prof. Dr. Osman Kükrer
Supervisor

Examining committee

1. Prof. Dr. Osman Kükrer

2. Prof. Dr. Mustafa K. Uyguroğlu

3. Asst. Prof. Dr. Reza Sirjani

ABSTRACT

Nowadays, researches have been carried out on reducing the total harmonics distortion when a voltage source inverter (VSI) is connected to the grid through a filter. LCL-filter reduces the harmonics contents when the switching frequencies are low and also the values of the inductance are low. Another advantage of LCL-filter is it has two possible current feedbacks that can be use for control. In this thesis, the current at the inverter side will be use for feedback control and no additional sensor is required. There was an observation that a natural damping term is present in the control loop, when the inverter side current is used for feedback control, instead of using active or passive damping technique. Steps to determine the values of the inductors at grid and inverter side are presented, so that ideal damping can be naturally obtained by using just the inverter side current control. When the steps to determine values of the inductors are not fulfilled, a notch filter with second order is used to extract the damping information from the converter current, then tuned the system damping with a compensation gain and due to its free of fundamental component, the compensation strategy will not cause an over modulation problem.

Simulation results for both strategy are shown using Matlab Simulink to prove the effectiveness of the proposed control strategy.

Keywords: Voltage source inverters (VSI), LCL filter, current control and resonance damping.

ÖZ

Günümüzde araştırmacılar, gerilim kaynaklı evirgeçlerin süzgeç üzerinden şebekeye bağlanması ile oluşan harmonikleri azaltma üzerinde çalışmaktadır. LCL-süzgeçin endüktans değerlerinin ve anahtarlama frekanslarının düşük olduğu durumlarda harmonik içeriği azalttığı bilinmektedir. LCL-süzgeçin diğer bir yararı da denetim için kullanabileceği iki akım geribeslemesine sahip olduğudur. Bu çalışmada sadece evirgeç akımı geribeslemeli denetim için kullanılacak, ve ek akım duyargasına gerek olmayacaktır. Aktif veya pasif bastırma yöntemi kullanmak yerine, geribeslemeli denetim için evirgeç akımı kullanılması durumunda denetim döngüsünde doğal bir bastırma teriminin var olduğu dikkate alınacaktır. Denetim için sadece evirgeç akımı kullanılması durumunda, ideal bastırma etkisini doğal olarak elde etmeye yönelik şebeke ve evirgeç tarafındaki endüktans değerlerinin hesaplanması için gerekli adımlar sunulacaktır. Endüktans değerlerinin hesaplanması sırasında şartların sağlanmaması durumunda, ikinci dereceden bir çentik süzgeç kullanılarak bastırma için gerekli bilgi evirgeç akımından elde edilebilir. Bu bilgi ile dizgenin bastırılması bir telafi kazancı ile ayarlanabilir. Akım bilgisinin esas bileşeni içermemesi nedeniyle bu yöntem aşırı kipleme sorununa yol açmaz. Her iki yöntem için Matlab Simulink ile elde edilen benzetim sonuçları, önerilen denetim yönteminin başarısını kanıtlamaktadır.

Anahtar Kelimeler: Gerilim kaynaklı evirgeçler, LCL süzgeç, akım denetim ve rezonans bastırma.

ACKNOWLEDGEMENT

Firstly, I appreciate God almighty for given me the strength and wisdom to complete this phase of my program.

My profound gratitude goes to Prof. Dr. OSMAN KÜKRER for his supervision, great support, advice and his guidance during my thesis.

I would like to thank the professors and instructors of Electrical and Electronics Engineering, Eastern Mediterranean University for their love and encouragements showered upon me during this program.

Special thanks also go to my family and my lovely friends for their prayers and support to see great success is achieved. I will be grateful forever for your love.

I would like to thank my lovely parents Mr and Mrs D.E Mogah for their spiritual, moral and financial support. Success is in my stride, because I have lovely parents like you by my side.

TABLE OF CONTENTS

LIST OF TABLES

LIST OF FIGURES

LIST OF SYMBOLS

f_s	Switching frequency
f_n	Nominal frequency
L_g	Grid-side inductor
L_{inv}	Inverter-side inductor
C_f	Filter capacitor
β	Ratio of resonance frequency and crossover frequency
V_g	Grid Voltage
V_{dc}	DC link Voltage
K_p	Proportional gain
ζ	Damping factor
I_g	Grid Current
τ_c	Integral time constant
w_{res}	Resonance frequency
w_c	Crossover frequency
I_{inv}	Inverter Current
I_g^*	Reference grid Current
I_c	Capacitor Current
k	Damping gain
S_n	Nominal power

LIST OF ABBREVIATIONS

VSI	Voltage source inverter
PWM	Pulse width modulation
DC	Direct current
AC	Alternating current
CSI	Current source inverter
THD	Total harmonic distortion

Chapter 1

INTRODUCTION

1.1 Background

Due to the increased demand on the renewable energy resources for generating electrical power, nowadays, renewable energy sources are connected to the utility grid through three-phase VSI. Usually, for smoothing the current entering the grid-side, a single inductor *L* is connected at the converter side. The disadvantage of using a single inductor may increase the cost and size of the passive filters and the system response may also be affected negatively [1], [16].

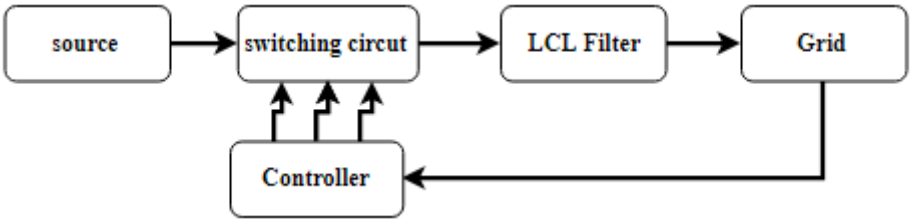

Figure 1: Block diagram of VSI.

In order to avoid this problem, some researchers use LCL-filter for three-phase voltage source inverter control, where it is found that LCL-filters decrease the current ripple[17] and its current can be sensed from the inverter-side or from the grid-side [2]. In this thesis the converter current was sensed and used for close-loop control [3]. Space vector pulse width modulation (SVPWM) was the best strategy used to control the inverter output voltage because it has been found that it has less

switching losses, less total harmonic distortion, effective dc bus utilization and easy to implement[15].

The main components of voltage source inverter are:

- DC source: This is a voltage source that produces dc voltage, and it is sent to the input of the switching circuit.
- Switching circuit: it is a bridge configuration that consists of power electronics switches. Three phase voltage source inverter consist of three paths with two switches in each. The signal from the PWM is used to control the switches.
- Filter: A passive filter is needed for connecting to the grid. The switching harmonics found at the VSI output are filtered using LCL-filter.
- Sensors: The output voltage or current of the inverter should be measured in order to establish a close-loop current or voltage control.
- Controller: This is used to bring about close loop operation in the inverter. It is designed to ensure stability in the close loop.
- Pulse width modulator: This is used to generate control signal for the switches. The most popular pulse width modulator (PWM) techniques are the sinusoidal PWM and space vector PWM.

1.2 Objectives

To investigate the natural damping characteristic of LCL- filters for three phase grid connected voltage source inverter.

A general design guideline for choosing the values of grid and converter side inductors, so that optimum damping can be naturally achieved.

Chapter 2

LITERATURE REVIEW

2.1 Inverter

Inverters are power electronics devices which transform direct current (DC) to alternating current (AC).

According to the output of the inverter, an inverter is known as voltage-controlled if the input is voltage source and current-controlled if input is current source [18]. In general, inverters are categorized into single-phase and three- phase inverter.

2.1.1 Voltage Source Inverter (VSI)

A constant voltage is realized at the DC side of VSI and the output current is changing with the load. For this reason an inductance is normally use to connect the VSI to the grid so as not to supply high current when there is no phase or voltage match between grid and inverter.

2.1.2 Current source inverter (CSI)

A constant current input is realized at the DC source of CSI and the voltage depends on the load. A capacitor is usually connected in parallel with the input DC source, acting as a protection filter.

2.2 Single-phase inverter

Single phase inverter is made-up of two kinds – half bridge inverter and full bridge inverter.

2.2.1 Half Bridge Inverter

It is the basic building block for three phase, full bridge and high order inverters. The capacitors (C_1 and C_2) are used to divide the DC source voltage into two parts. The capacitors are usually large and they are used to provide neutral point. If the upper switches are on, the lower switches must be off, and vice-versa. The two switches (Q_1 and Q_2) have to be complementary. V_{out} is equal to $V_s/2$ throughout the positive half cycle of the output voltage and $-V_s/2$ during the negative half cycle.

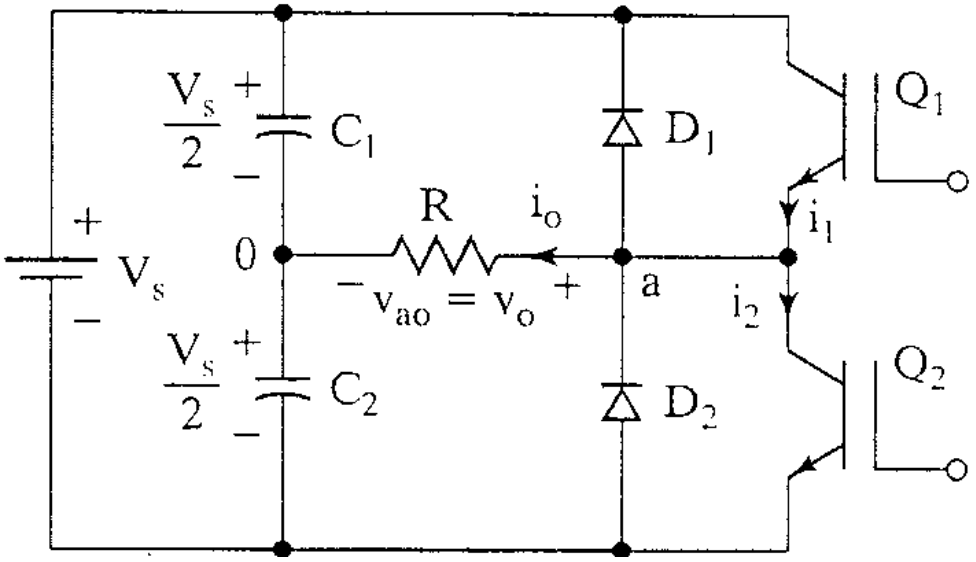

Figure 2: Single phase half bridge inverter [18].

2.2.2 Single phase full bridge inverter

A single phase full bridge inverter is made-up of two half bridges as shown in Figure 3. The output voltage is not referred to the neutral point, so it's not necessary to provide two capacitors, but it can be used to provide neutral point.

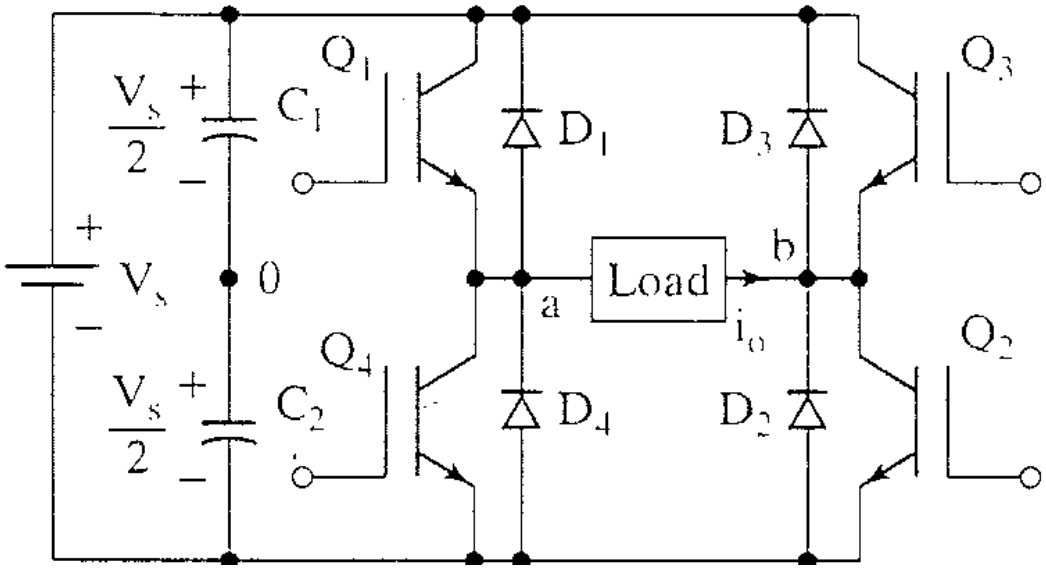

Figure 3: Single phase full bridge inverter [18].

2.3 Three Phase Inverter

These types of inverter consist of three legs in which, if the upper switches are on then the lower switches must be off. The output voltage is related to the states of the switches and DC voltage applied at the input. In conclusion the output voltage does not depend on the applied load [19].

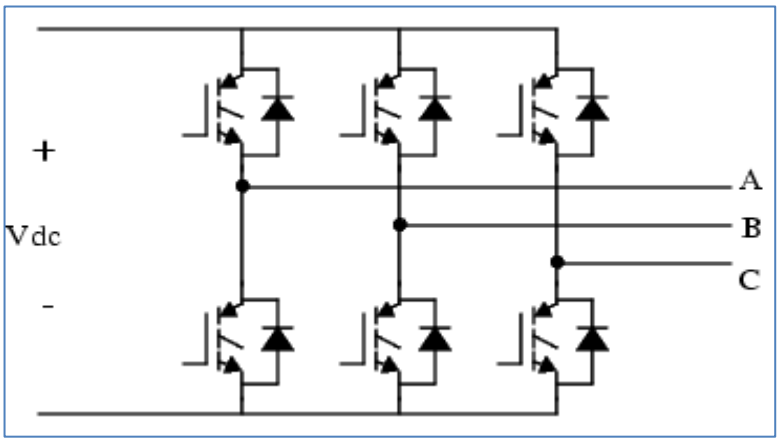

Figure 4: Three phase inverter [19].

2.4 Space vector pulse width modulation

The SVPWM has advantage over Sinusoidal PWM (SPWM) in terms of good use of dc bus voltage, low current ripple and reduced switching frequency. The SVPWM is chosen to be a better technique for implementing PWM, as it provides a lagre range for fundamental component for the output voltage and more effective in suppressing the THD of the whole system.

To carry out the SVPWM, the voltage can be transformed from abc reference frame to $\alpha\beta$ stationary frame [7]

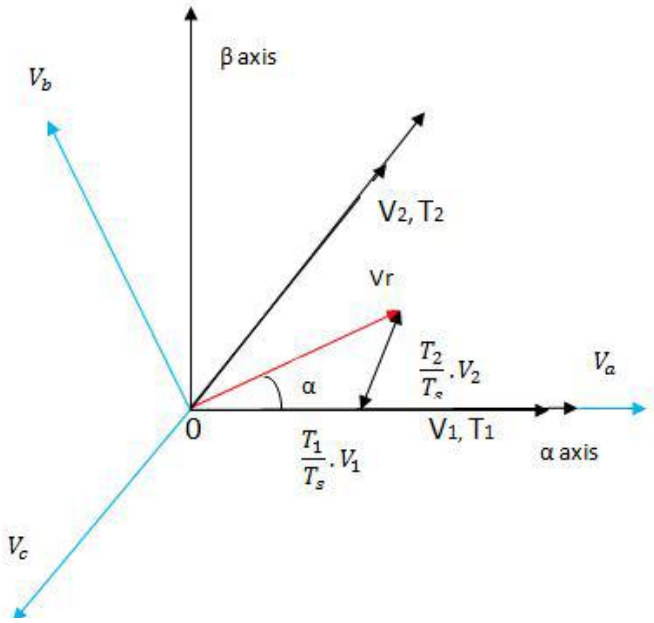

Figure 5: Reference vector in $\alpha\beta$ frame [7].

2.5 Popular damping methods for LCL-filter resonance

There are two popular methods used for damping the resonance of LCL-filter

- Active damping
- Passive damping

2.5.1 Active damping

For active damping, a virtual resistor is connected in series or in parallel with the capacitor or the inductor of the filter. There are four possible ways to connect the virtual resistor, according to [8]. Figure 6 shows the equivalent circuit per phase at the grid side. I_{inv} is taken to be the reference current and it is the fundamental component of the phase output current of the VSI. Figure 7 shows the block diagrams of the system using the four types of virtual resistor method.

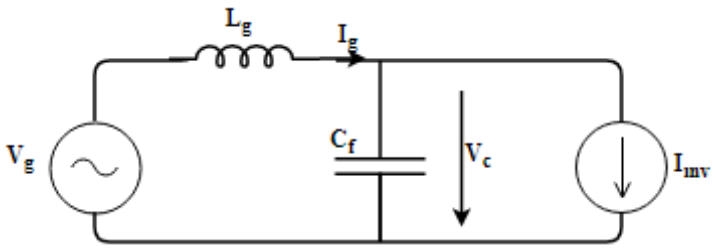

Figure 6: Equivalent circuit per phase at the grid side.

If the capacitor or inductor is parallel with the connected virtual resistor, an additional voltage sensor is needed and if the capacitor or inductor is in series with the connected virtual resistor, an additional current sensor is needed.

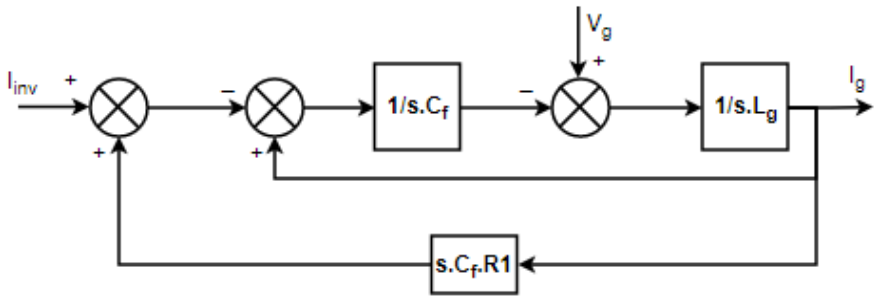

(a) R_1 Connected in series with filter inductance.

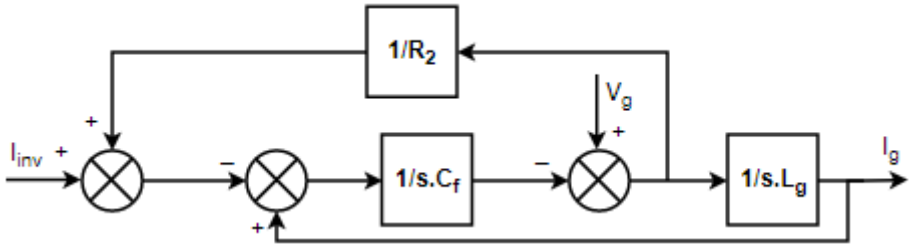

(b) R_2 Connected in parallel with filter inductance.

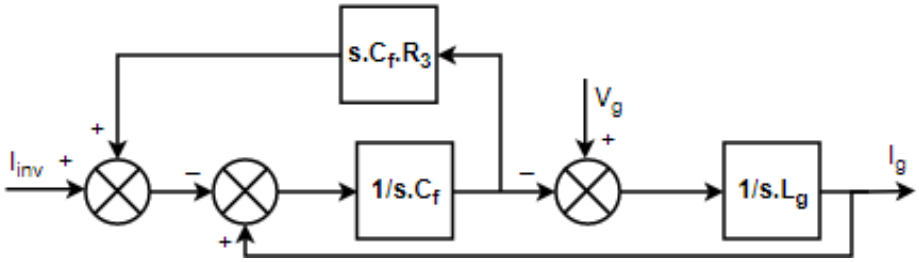

(c) R_3 Connected in series with filter capacitance.

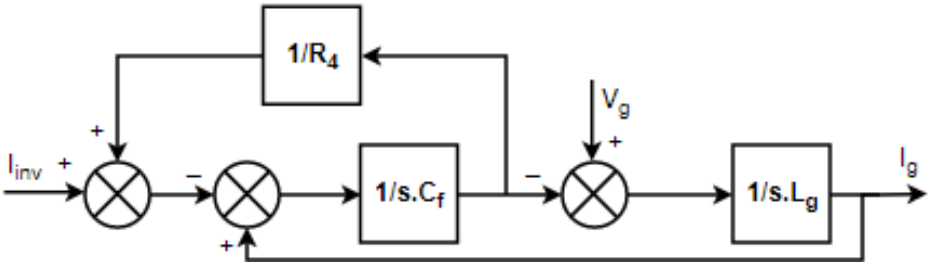

(d) R_4 Connected in parallel with filter capacitance.

Figure 7: Block diagrams for using types of virtual resistor method.

2.5.2 Passive damping

Passive damping is another method of damping the resonance of a filter. It is achieved by connecting a physical resistor in series or in parallel with the capacitor or the inductor of the filter. Figure 8 shows the various ways the resistor can be connected.

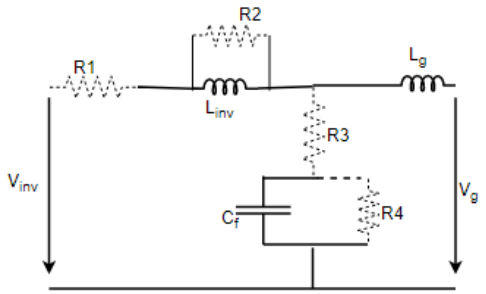

Figure 8: Possible positions for the resistor.

Chapter 3

SYSTEM MODELING AND DESCRIPTION

Figure 9 shows an overall circuit diagram of a grid connected three-phase inverter via an LCL-filter. The assumption made here is by neglecting the resistances of all inductors and capacitor, the grid voltages contain only fundamental positive sequence component, and they are presented as short circuits without any impedance when carrying out harmonic analysis and system stability.

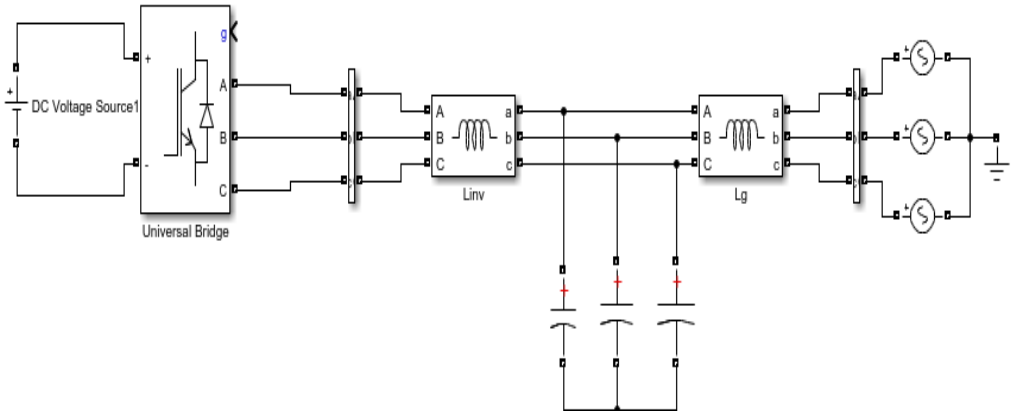

Figure 9: Grid connected three-phase inverter via an LCL-filter.

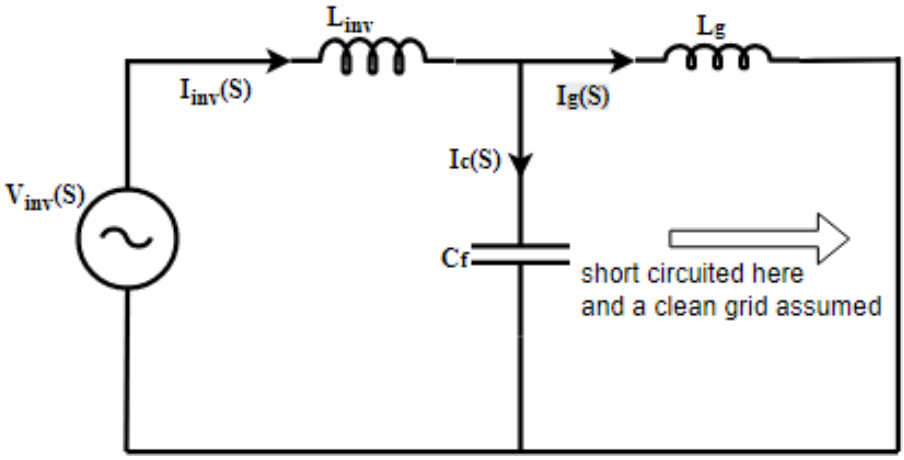

Figure 10: Equivalent circuit per phase for stability analysis.

The grid-connected three-phase inverter via an LCL-filter is reduced as shown in Figure 10. The transfer function of plant model $G_{plant}(s)$ is derived in s-domain, by applying KCL rule in the circuit:

$$I_{inv}(s) = I_c(s) + I_g(s) \tag{1}$$

$$V_{inv}(s) = L_{inv} I_{inv} s + \frac{I_{inv}}{C_f s} - \frac{I_g}{C_f s} \tag{2}$$

$$I_c(s) = L_g C_f I_g s^2 \tag{3}$$

By substituting Eq.(3) into Eq.(1), I_{inv} can be expressed as:

$$I_{inv}(s) = (L_g C_f s^2 + 1) I_g \tag{4}$$

By substituting Eq. (4) into Eq. (2) , the $G_{plant}(s)$ can be written as:

$$G_{plant}(s) = \frac{I_g(s)}{V_{inv}(s)} = \frac{1}{L_g L_{inv} C_f s^3 + \left(L_{inv} + L_g\right) s} \tag{5}$$

$$\frac{I_c(s)}{I_g(s)} = L_g C_f s^2 \tag{6}$$

Where V_{inv} I_{inv}, I_c and I_g are the inverter voltage, inverter current, capacitor current and grid current.

3.1 Current Feedback

When LCL-filter is used for connecting an inverter to a grid, it is observed that it's easier to sense the grid current or converter current, unlike L-filter where the only sensing current is the inductor current. LCL-filter has two possible current feedbacks.

3.1.1 Grid Current Feedback

The control block diagram of LCL-filter with the feedback from the grid current is illustrated below as Figure 11.

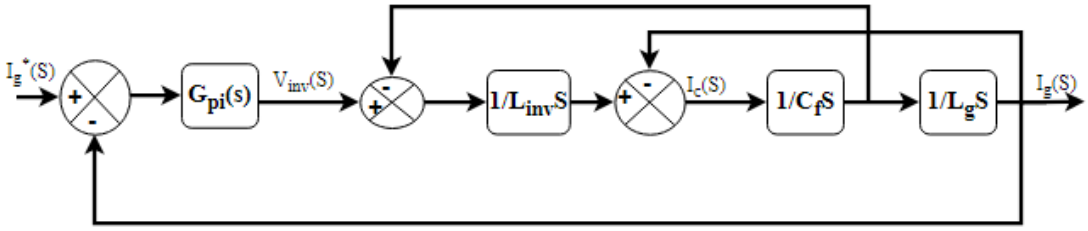

Figure 11: Block diagram of grid current feedback control.

$$G_{pi} = K_p V_{dc}\left(1+\frac{1}{\tau_c s}\right) \tag{7}$$

Equation (7) is the proportional-integral (PI) controller in *dq* reference frame, where K_p, V_{dc}, and τ_c represent the proportional gain, dc-link voltage and integral time constant of the PI controller.

The block diagram is analyzed to determine the open-loop transfer function of the system:

$$\frac{I_g(s)}{I_g^*(s)-I_g(s)} = G_{pi}(s)G_{plant}(s) = \frac{K_p V_{dc}\left(s+\frac{1}{\tau_c}\right)}{L_g L_{inv} C_f s^4 + \left(L_{inv}+L_g\right)s^2} \tag{8}$$

The stability of the close loop system is difficult to achieve due to the absence of the third order term in the characteristic equation. Even if a passive element is included, a well damped system can't be achieved.

3.1.2 Converter Current Feedback

Figure 12 shows that the feedback control can be sensed from the converter current. The *q*- axis current reference is set to $w_n C_f V_g$ instead of zero, since the grid current can't be controlled directly, where w_n is the fundamental angular frequency, C_f is filter capacitor and V_g is the grid voltage. To enable unity power factor is achieved before the grid terminal.

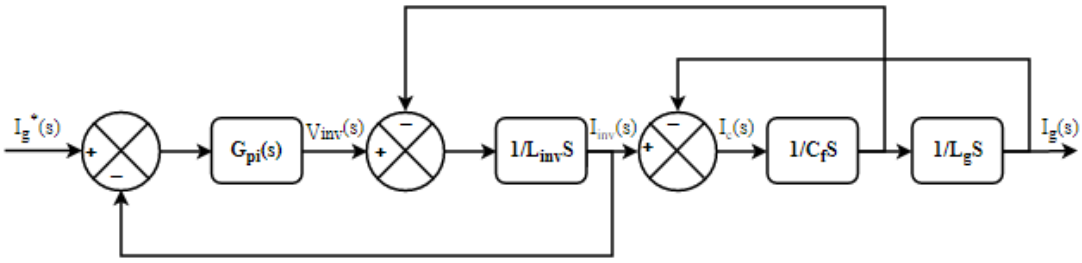

Figure 12: Block diagram of inverter side current feedback control.

For easy performance of open loop analysis, Figure 12 is modified to Figure 13.

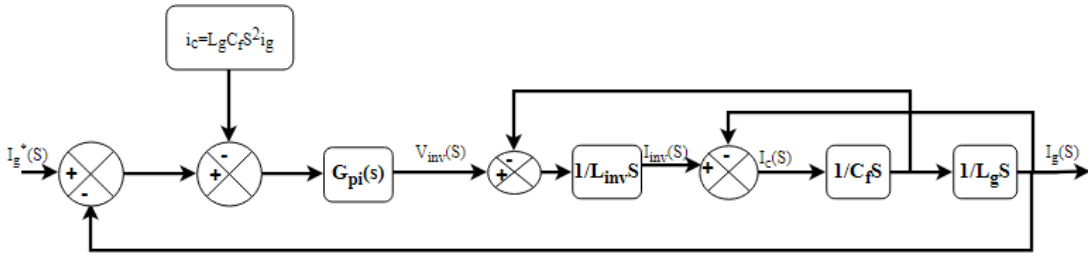

Figure 13: Corresponding block diagram of inverter side current feedback control.

From Eq. (1) the inverter side current is represented as the addition of capacitor current and grid current which is shown in Figure 13. When Figure 12 is compared with Figure 13 we can see that with including i_c term to the forward path, inverter side current feedback and grid side current feedback are equivalent. It is easier to obtain the open loop transfer function from the corresponding converter feedback control.

$$\frac{I_g(s)}{I_g^*(s)-I_g(s)-I_c(s)} = G_{pi}(s)G_{plant}(s) = \frac{K_pV_{dc}\left(s+\frac{1}{\tau_c}\right)}{L_gL_{inv}C_fs^4+\left(L_{inv}+L_g\right)s^2} \tag{9}$$

By Substituting Eq. (6) to Eq. (9) it can easily been seen that Eq. (10) contains the third-term, in which two poles fix at the origin, while the other two poles are moved into the left side of the real axis, which would provide damping.

$$\frac{I_g(s)}{I_g^*(s)-I_g(s)} = \frac{K_p V_{dc}\left(s+\frac{1}{\tau_c}\right)}{L_g L_{inv} C_f s^4 + K_p V_{dc} L_g C_f s^3 + \left(\frac{K_p V_{dc} L_g C_f}{\tau_c} + L_{inv} + L_g\right)s^2} \quad (10)$$

Tuning is required to reach this case:

$$\frac{K_p V_{dc}}{L_{inv}} = 2\varsigma w_{res} = 2\varsigma\sqrt{\frac{K_p V_{dc} L_g C_f / \tau_c + L_{inv} + L_g}{L_{inv} L_g C_f}} \quad (11)$$

Where w_{res} is the undamped resonance frequency, was substituted as the square-root term. The resonance frequency is not fully depending on the PI controller, so

$w_{res} \approx \sqrt{\frac{L_{inv}+L_g}{L_{inv}L_g C_f}}$ where $K_p V_{dc} L_g C_f / \tau_c = 0$ from Eq. (11)

3.2 Ideal Damping Control of LCL Filter

The phase response of L-filter and LCL-filter is quite different, L-filter has a maximum phase lag of 90 degree, while that of an LCL-filter always surpass 90 degree. If the operating frequency and the damping factor increases the phase increases for LCL-filter. Due to the phase differences of LCL-filter, the damping factor of LCL resonance is optimally tuned. In [1], it is suggested that ω_c should be selected as a fraction of the undamped resonance frequency [20]. When optimum damping of the LCL resonance was considered ($\zeta = 0.7$), the crossover can be determine from equation (12).

$$w_c = \beta w_{res} \quad (12)$$

Where β = 0.3

The system phase margin depends on the ratio of the crossover frequency to resonance frequency β and it's damping factor ζ as shown below:

$$\varphi_{LCL} = \frac{\pi}{2} + \arctan\left(\frac{2\beta\zeta}{1-\beta^2}\right) \quad (13)$$

In [4] the relationship between K_p and w_c is determined as follows

$$K_p = \frac{w_c \left(L_{inv} + L_g \right)}{V_{dc}} \tag{14}$$

For ensuring the stability of the closed loop control system, the value of the proportional gain should be low and for this reason the system bandwidth is designed in a low frequency range.

Combining Eq. (11) and (14) gives:

$$\frac{w_c \left(L_{inv} + L_g \right)}{L_{inv}} = 2\zeta w_{res} \tag{15}$$

Substituting Eq. (12) into (15) gives the relationship between the inverter inductor and the grid inductor.

$$\frac{L_{inv}}{L_g} = \frac{\beta}{2\varsigma - \beta} \tag{16}$$

If equation (16) is satisfied, the proportional gain of the PI controller won't affect the ideal damping performance. The filter capacitor should be determined first in LCL-filter because from equation (16), the filter capacitor does not influence the performance of resonance damping.

When the inverter and grid inductors are chosen to be equal, equation (16) won't be satisfied but the LCL-filter may establish better harmonic attenuation. Additional damping term should be included to adjust the second term coefficient of equation (10), in order to ensure the effectiveness of optimum damping regardless of the ratio between the inductors. The capacitor current is measured to achieve a tunable damping factor and compared with the current reference with a proportional gain *k* as show in Figure 14.

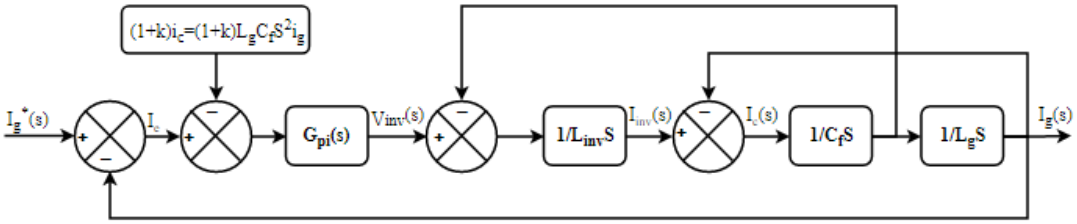

Figure 14: Improved corresponding inverter side current feedback control.

This leads to following equation

$$\frac{I_g(s)}{I_e(s)-(1+k)I_c(s)} = G_{pi}(s)G_{plant}(s) = \frac{K_pV_{dc}\left(s+\frac{1}{\tau_c}\right)}{L_gL_{inv}C_fs^4+\left(L_{inv}+L_g\right)s^2} \tag{17}$$

The open-loop gain is determined by substituting Eq. (6) into (17) as shown in (18)

$$\frac{I_g(s)}{I_e(s)} = \frac{K_pV_{dc}\left(s+\frac{1}{\tau_c}\right)}{L_gL_{inv}C_fs^4+(1+k)K_pV_{dc}L_gC_fs^3+\left[(1+k)\frac{K_pV_{dc}L_gC_f}{\tau_c}+L_{inv}+L_g\right]s^2} \tag{18}$$

The denominator's second term in (18) represents the damping factor for LCL-filter and a relationship shown in (19) should be satisfied to establish ideal damping control.

$$\frac{(1+k)K_pV_{dc}}{L_{inv}} = 2\zeta w_{res} \tag{19}$$

For calculating the feedback gain of i_c equation (14) is substituted into (19)

$$k = \frac{2\zeta L_{inv}}{\beta\left(L_{inv}+L_g\right)} - 1 \tag{20}$$

3.3 Space vector pulse width modulation (SVPWM)

The signal generated by the PWM is sent to the input of the switching circuit. For two levels VSI there are eight switching topologies according to various vectors. There are six sectors and each has 60 degree span. The six sectors and their

respective angles are show in Table 1 below. A space vector for a set of three-phase voltages can be represented as:

$v_a = V_m \sin(\omega t)$

$v_b = V_m \sin(\omega t - 120^o)$

$v_c = V_m \sin(\omega t - 240^o)$

Consider the three phase voltage (V_a ,V_b and V_c) with 120 degree apart, the three phase voltage is transformed to $\alpha\beta$ component and after that V_α , V_β , V_{ref} and α can be determined.

$$V_\alpha = \frac{2}{3}\left(V_a - \tfrac{1}{2}V_b - \tfrac{1}{2}V_c\right) \quad (21)$$

$$V_\beta = \frac{2}{3}\left(\tfrac{\sqrt{3}}{2}V_b - \tfrac{\sqrt{3}}{2}V_c\right) \quad (22)$$

$$|V_{ref}| = \sqrt{V_\alpha^2 + V_\beta^2} \quad (23)$$

$$\alpha = \tan^{-1}\left(\frac{V_\beta}{V_\alpha}\right) \quad (24)$$

Table 1: sectors and their respective angle.

Sectors	V_{ref} **position**
1	$0 < wt < 60$
2	$60 < wt < 120$
3	$120 < wt < 180$
4	$180 < wt < 240$
5	$240 < wt < 300$
6	$300 < wt < 360$

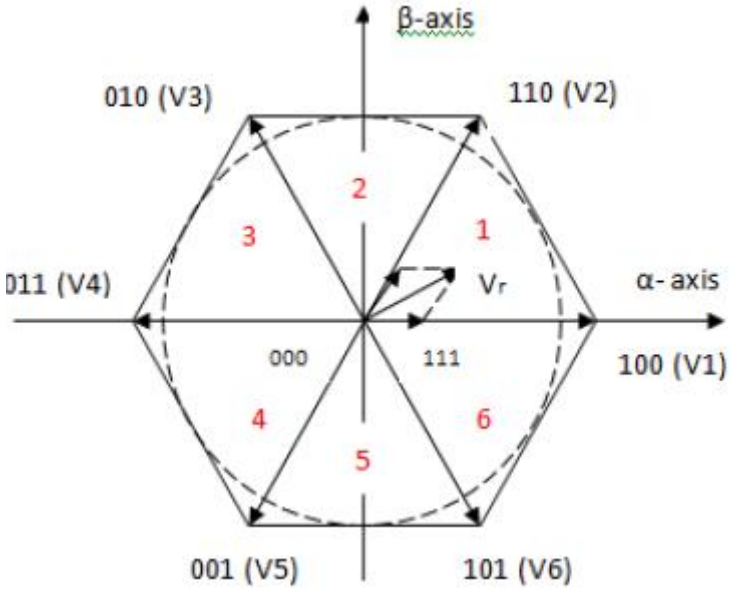

Figure 15: Switching vectors and sectors [7].

By using equation (25), (26) and (27) the switching time for each sector is determined as

$$T_1 = \frac{\sqrt{3}}{V_{dc}}.|V_{ref}|.T_s.\sin\left(\frac{n}{3}\pi - \alpha\right) \tag{25}$$

$$T_2 = \frac{\sqrt{3}}{V_{dc}}.|V_{ref}|.T_s.\sin\left(\alpha - \frac{n-1}{3}\pi\right) \tag{26}$$

$$T_0 = T_s - T_1 - T_2 \tag{27}$$

Where $T_s = \frac{1}{f_s}$, n is the number of sector, and α is the angle of the reference voltage.

The switching time duration for all sectors is show in Table 2:

Table 2: The switching time duration for all sectors

Sectors	T_0	T_1	T_2
1	$T_s - T_1 - T_2$	$T_s . \frac{V_{ref}}{\frac{2}{3}V_{dc}} \sin\left(\frac{\pi}{3} - \alpha\right)$	$T_s . \frac{V_{ref}}{\frac{2}{3}V_{dc}} \sin(\alpha)$
2	$T_s - T_1 - T_2$	$T_s . \frac{V_{ref}}{\frac{2}{3}V_{dc}} \sin\left(\frac{2\pi}{3} - \alpha\right)$	$T_s . \frac{V_{ref}}{\frac{2}{3}V_{dc}} \sin\left(\alpha - \frac{\pi}{3}\right)$
3	$T_s - T_1 - T_2$	$T_s . \frac{V_{ref}}{\frac{2}{3}V_{dc}} \sin(\pi - \alpha)$	$T_s . \frac{V_{ref}}{\frac{2}{3}V_{dc}} \sin(\alpha - \pi)$
4	$T_s - T_1 - T_2$	$T_s . \frac{V_{ref}}{\frac{2}{3}V_{dc}} \sin\left(\frac{4\pi}{3} - \alpha\right)$	$T_s . \frac{V_{ref}}{\frac{2}{3}V_{dc}} \sin(\alpha - \pi)$
5	$T_s - T_1 - T_2$	$T_s . \frac{V_{ref}}{\frac{2}{3}V_{dc}} \sin\left(\frac{5\pi}{3} - \alpha\right)$	$T_s . \frac{V_{ref}}{\frac{2}{3}V_{dc}} \sin\left(\alpha - \frac{4\pi}{3}\right)$
6	$T_s - T_1 - T_2$	$T_s . \frac{V_{ref}}{\frac{2}{3}V_{dc}} \sin(2\pi - \alpha)$	$T_s . \frac{V_{ref}}{\frac{2}{3}V_{dc}} \sin\left(\alpha - \frac{5\pi}{3}\right)$

Chapter 4

SIMULATION RESULTS

For the system to have acceptable bandwidth control the resonance frequency should be about 30 times the fundamental frequency. It is suggested by Liserre et al. [3] that switching frequency should be at least twice that of the resonance frequency, and this means that the switching frequency in this system should be greater than 3 kHz. The system base values Z_b, L_b and C_b are calculated below:

$$Z_b = \frac{V_g^2}{S_n} = 9.6\Omega$$

$$L_b = \frac{Z_b}{w_n} = 31mH$$

$$C_b = \frac{1}{w_n Z_b} = 332\mu F$$

Table 3: Grid connected three phase VSI parameters.

Parameters	Values
f_s	5kHz
f_n	50Hz
V_g	120V
K_p	0.06
V_{dc}	260V
τ_c	0.005
K	1.2
L_g	3.19mH
L_{inv}	0.87mH
C_f	15µF
S_n	1.5kVA

4.1 Design of LCL-filter based on proposed guideline

From Eq. (11) we deduced that $w_{res} \approx \sqrt{\frac{L_{inv}+L_g}{L_{inv}L_gC_f}} = \frac{1}{\sqrt{L_pC_f}}$

Where $L_p = \frac{L_{inv}L_g}{L_{inv}+L_g}$

w_{res} can be calculated from the value of parallel inductance and filter capacitance. [3] recommended that the resonance frequency should be thirty times the nominal frequency and the value on filter capacitance should be limited to 4.5% of the base capacitance.

$$w_{res} = \frac{1}{\sqrt{L_pC_f}} \tag{28}$$

Where, $L_p = \frac{\left(1/w_{res}\right)^2}{C_f}$, $w_{res} = 30w_n$ and $C_f = 15\mu F$

For $\beta = 0.3 and\ \zeta = 0.7$, the inverter and grid side inductance are computed below

$$L_{inv} = \frac{2\zeta}{2\zeta - \beta}L_p$$

$$L_g = \frac{2\zeta}{\beta}L_p \tag{29}$$

Using Eq. (29), the inverter-side and grid-side inductor was determined as given in Table 3.

All the parameters are chosen to be the same as in Table 3 and Matlab Simulink was used to verify that optimum damping can naturally be satisfied using one current sensor, therefore the converter current used as a feedback without any additional damping technique. There is no current overshoot and the inverter can respond very fast when step response from 5 to 10A is used as the reference current. Figure 16 shows the result of the simulation. The THD of the grid current was measured to be

0.8% meaning the resonance was successfully suppressed. Its harmonic spectrum is shown in figure 17.

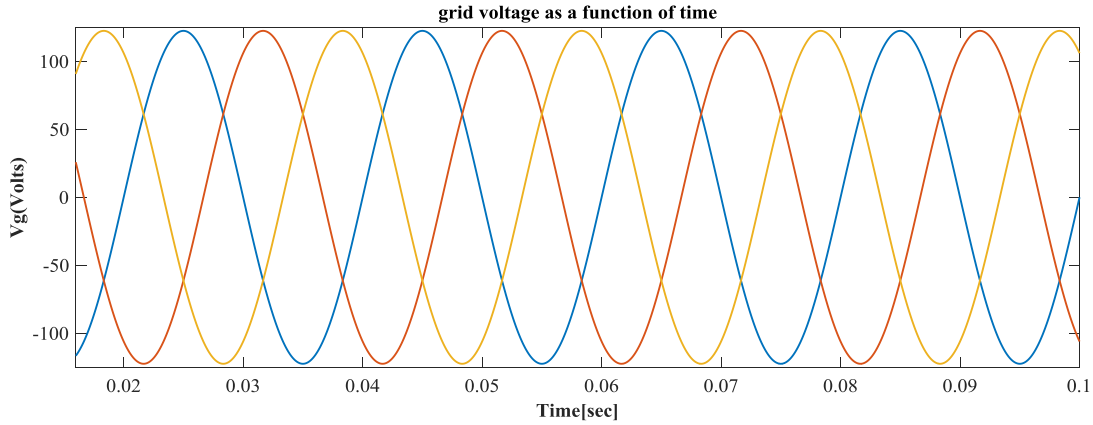

(a)

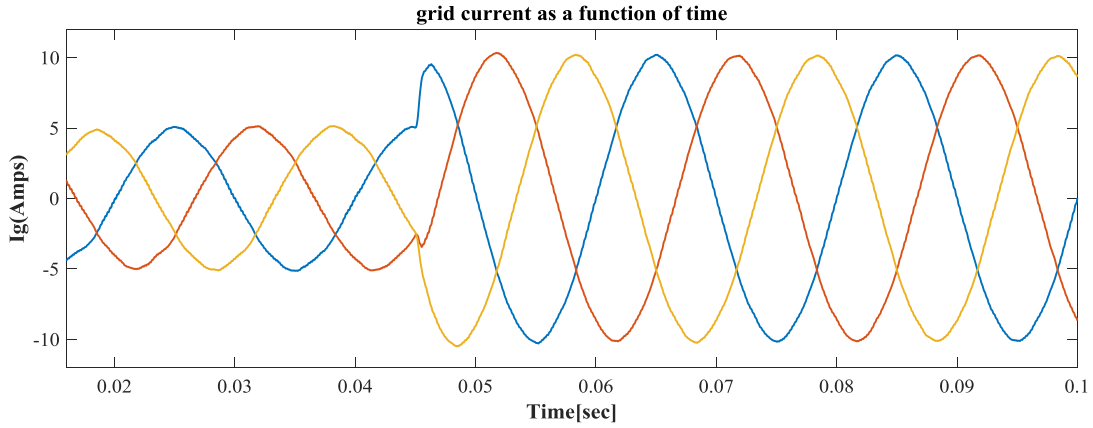

(b)

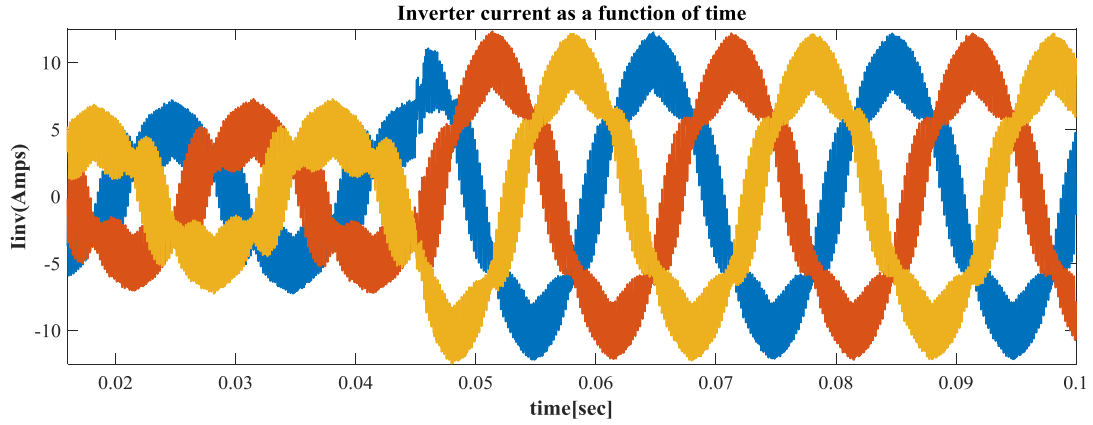

(c)

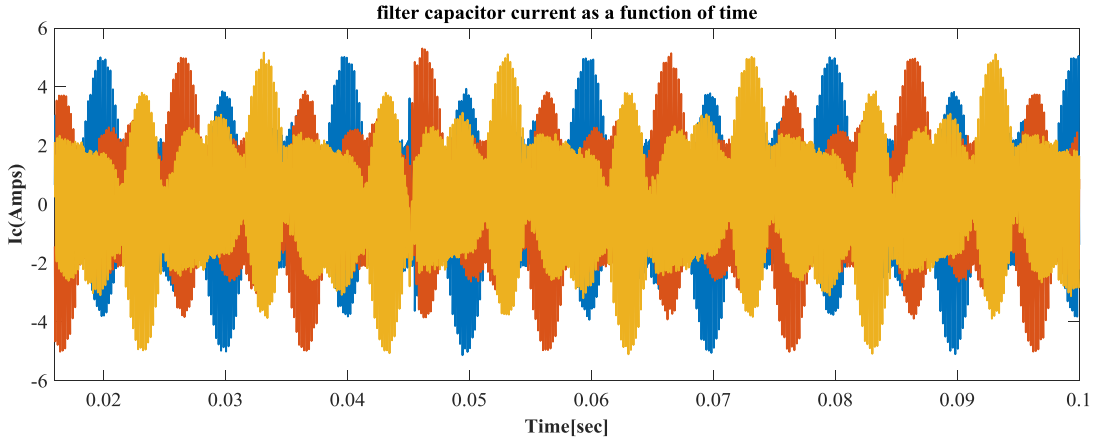

(d)

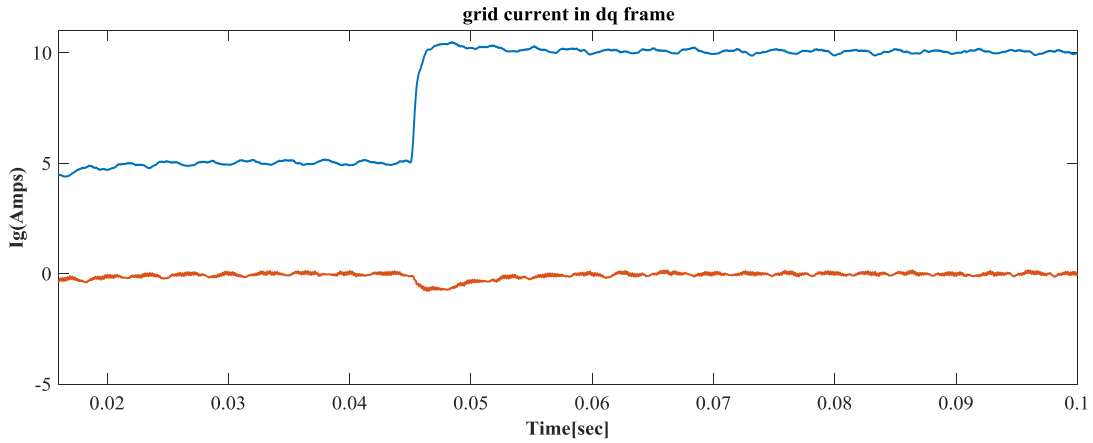

(e)

Figure 16: Simulated results with correct inductors values (a) grid voltage (b) grid current (c) inverter current (d) filter capacitor and (e) grid current in dq frame.

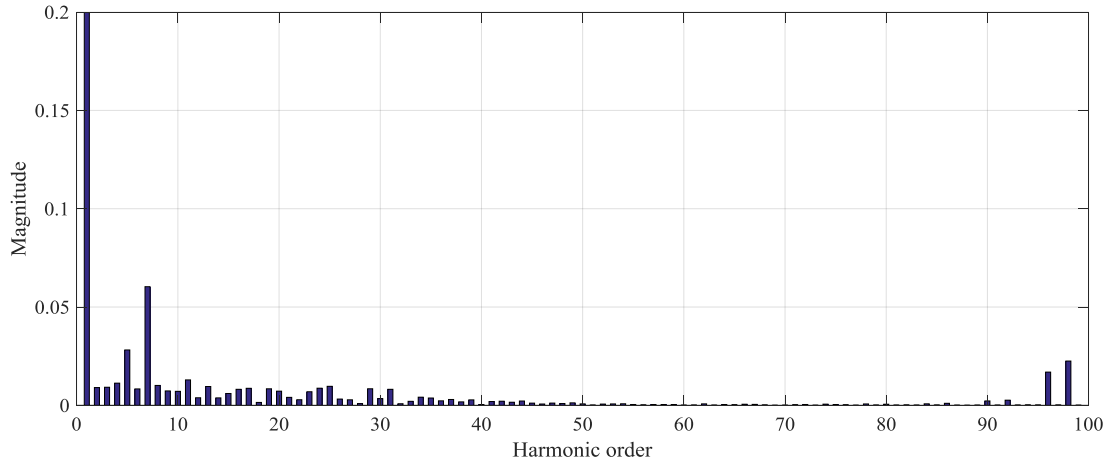

Figure 17: Harmonic spectrum of grid current using inverter current feedback control

The values of inductor were interchanged (L_{inv}=3.19mH and L_g=0.87mH) in other to verify how true (16) can be, the bandwidth and filter capacitance are kept the same. Figure 18 shows that the LCL-filter resonance is not properly damped, which causes oscillations due to the fact that (16) is unsatisfied.

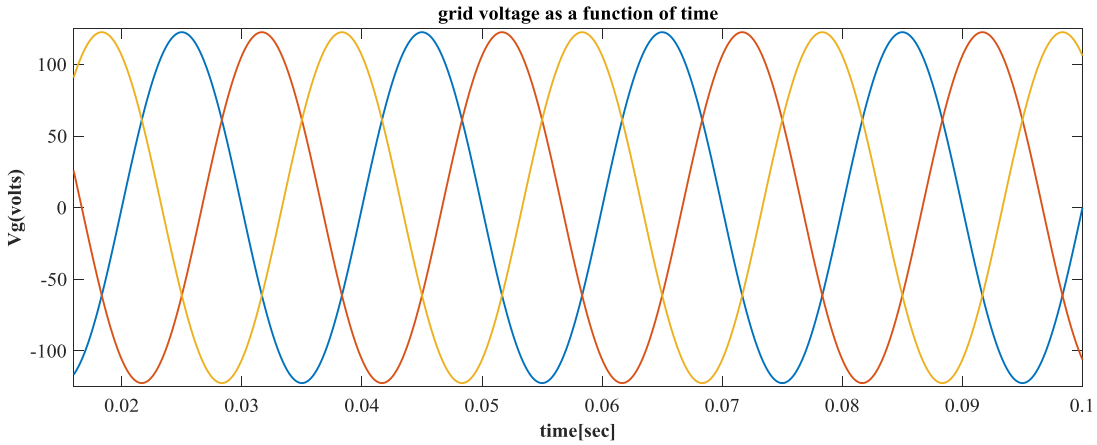

(a)

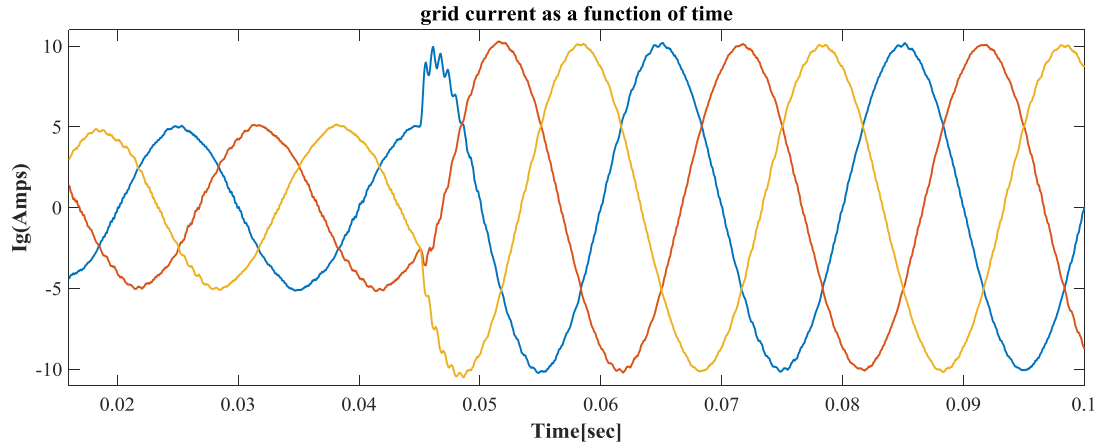

(b)

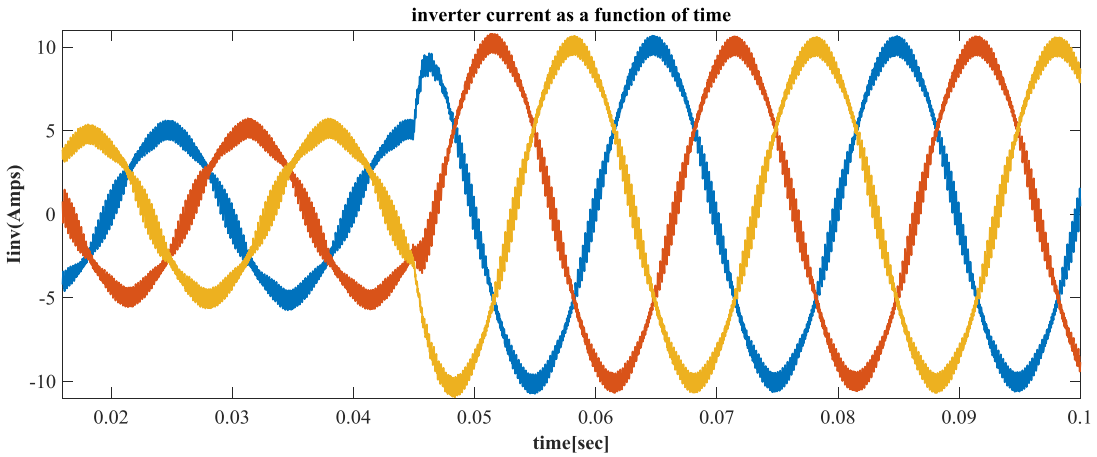

(c)

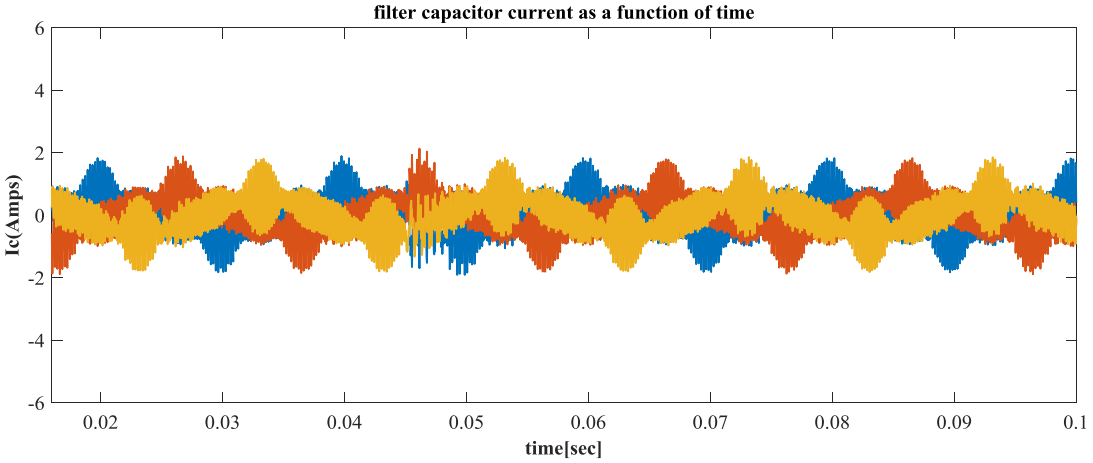

(d)

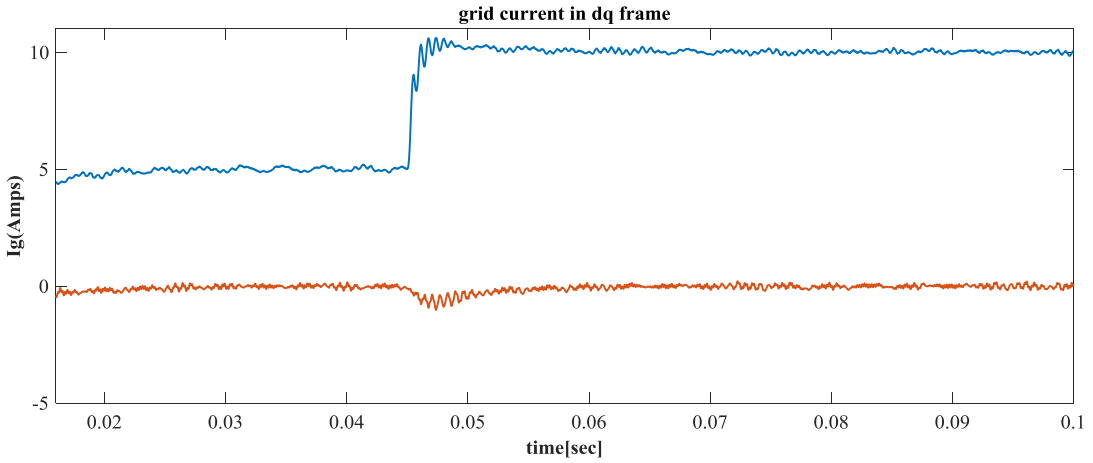

(e)

Figure 18: Simulated results for with incorrect inductors values (a) grid voltage (b) grid current (c) inverter current (d) filter capacitor current and (e) grid current in *dq* frame.

4.2 Equivalent values of inverter and grid inductor

If the predetermined values of LCL filter couldn't achieve the design criterion presented in (16), the optimum damping could be achieved with suitable feedback control of capacitor currents as proposed in [5],[6],[9] and [10]. All other values are same, now grid inductor is selected to be equal to inverter inductor (L_{inv}=L_g=1.36mH) to reduce switching harmonics. The converter current was sensed and used for the feedback control because the harmonic component present in it

could achieve the stability of the system without using any other damping techniques. All the harmonics in i_{inv} are suppressed by the filter capacitor; the filtered i_{inv} is approximated as i_c. A notch filter with second order was used to extract i_c from i_{inv}. By multiplying equation (30) with the damping gain which can be calculated from equation (20) i_c can be simply realized.

$$H(s) = \frac{s^2 + w_n^2}{s^2 + \left(w_n / Q\right)s + w_n^2} \tag{30}$$

Where w_n is the angular frequency and Q is chosen to be 0.7

The distorted three phase grid voltage by fifth and seventh harmonics becomes sixth harmonic in the synchronous frame. This can be resolved by adding harmonic controller (31) in parallel with the PI controller which cancels distortions in the line current as discussed in [11] and [12].

$$G_r = \frac{K_r s}{s^2 + \left(6w_n\right)^2} \tag{31}$$

Where K_r is the same as the integral gain of PI controller [13], [14].

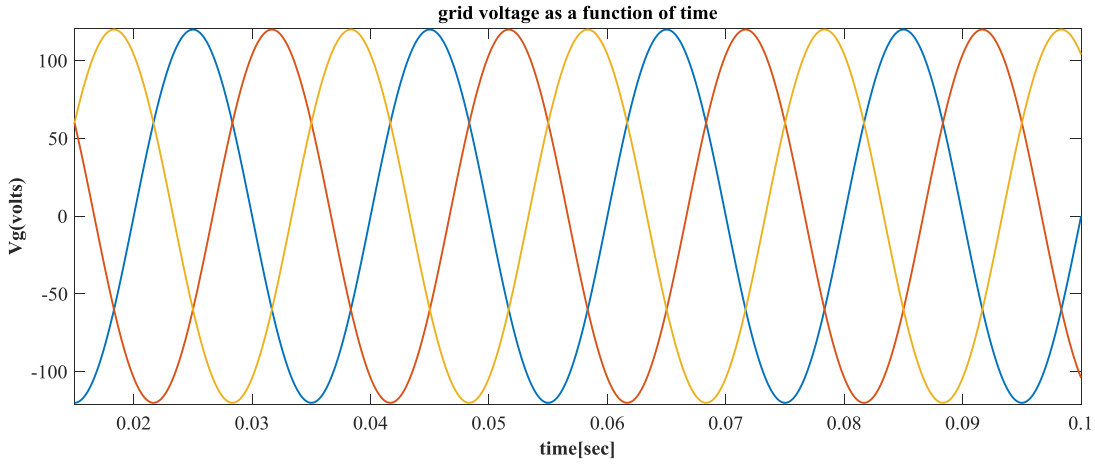

(a)

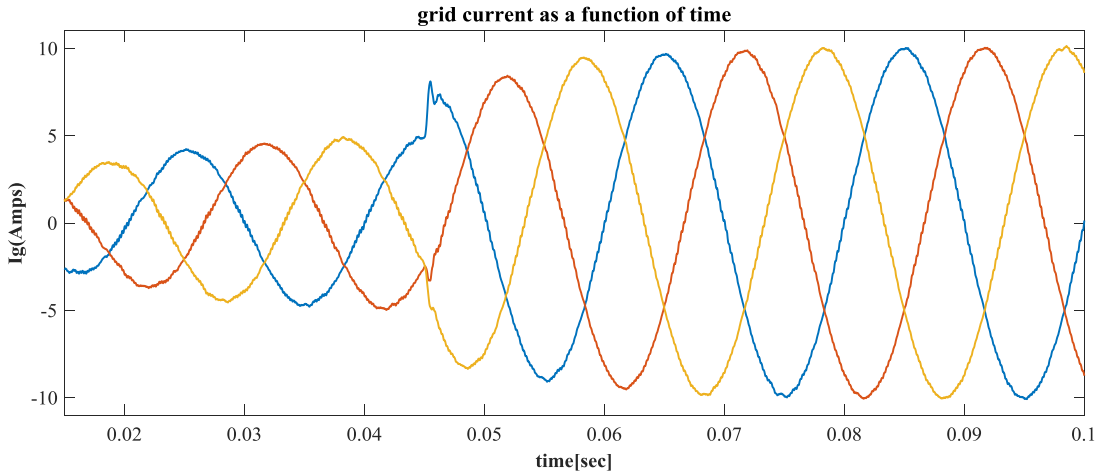
grid current as a function of time
Ig(Amps)
time[sec]

(b)

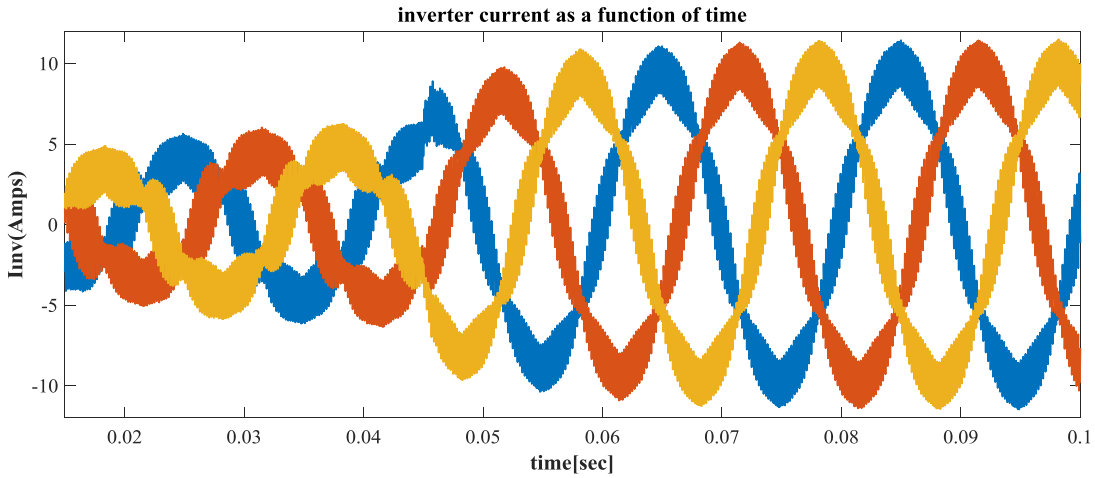
inverter current as a function of time
Inv(Amps)
time[sec]

(c)

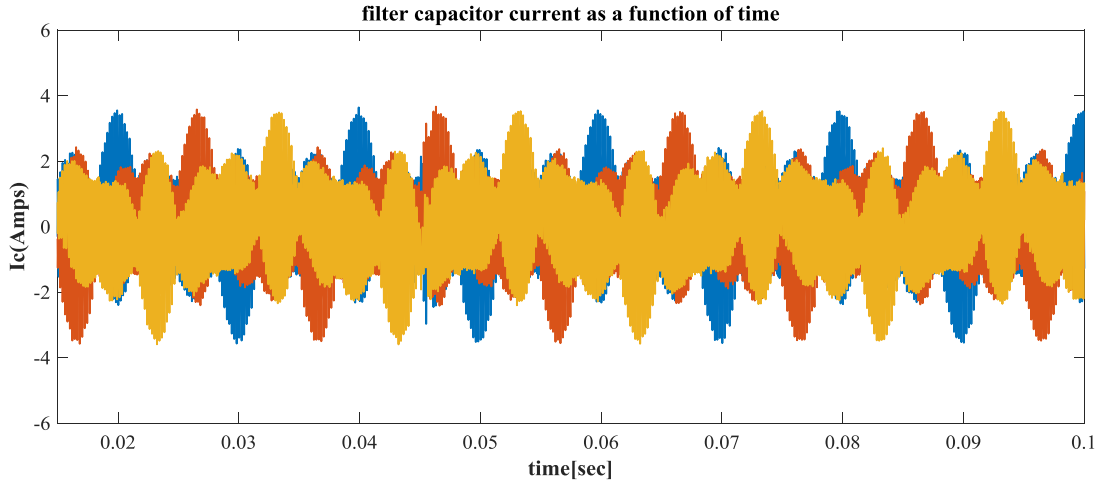
filter capacitor current as a function of time
Ic(Amps)
time[sec]

(d)

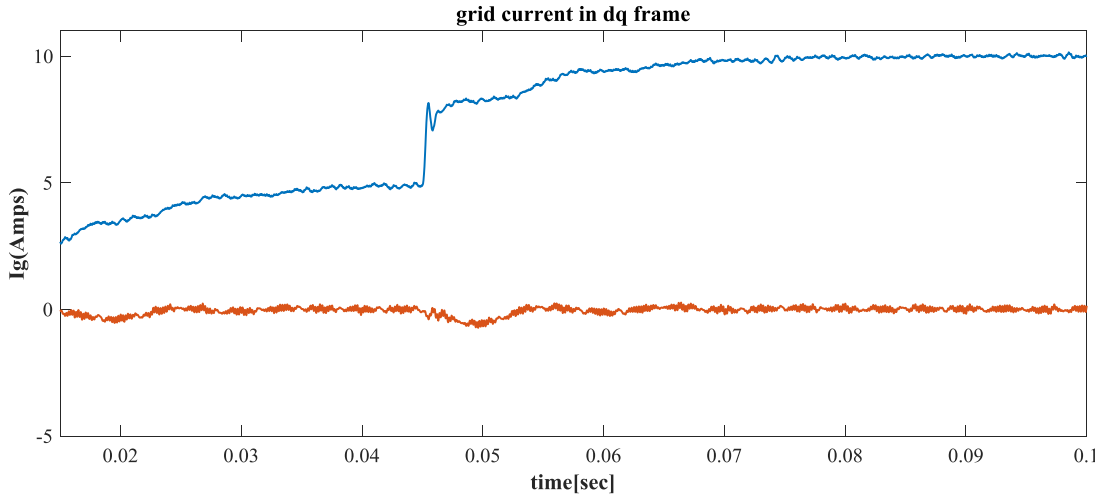

(e)

Figure 19: Simulated results with equal inductors values (a) grid voltage (b) grid current (c) inverter current (d) filter capacitor current and (e) grid current in *dq* frame

4.3 Grid Current measured for feedback

The grid current was measured and used for feedback; there is no natural damping term in the grid side, the simulation waveform for grid current when VSI is in operation without any damping term is show in Figure 20. So a passive damping was done using a 2Ω resistor in series with the capacitor. From Figure 21 it is clear that the resistance is not sufficient enough to damp the grid current and causes transient oscillations. The THD of the grid current was measured to be 1.5% meaning the resonance was not successfully suppressed. Its harmonic spectrum is shown in Figure 22.

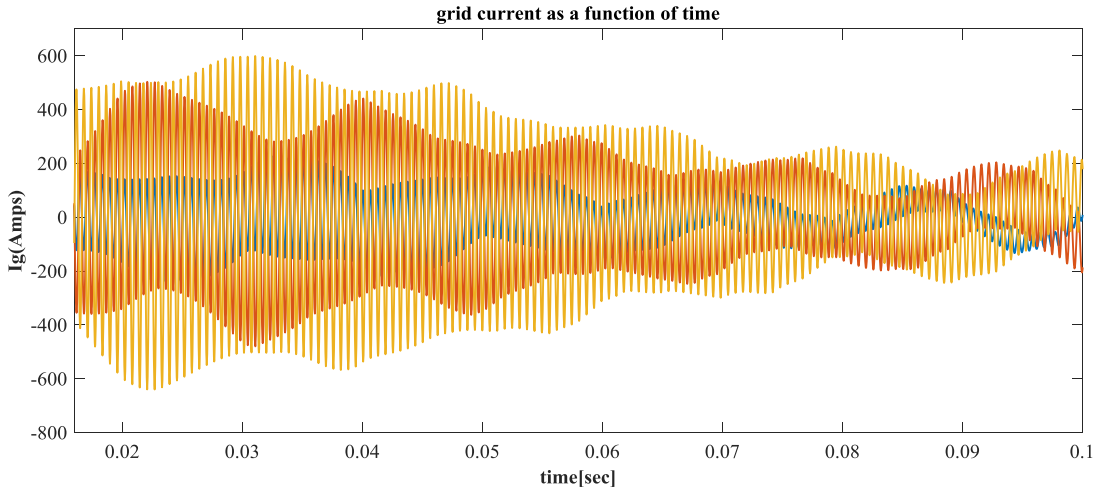

Figure 20: simulation waveform for grid current when VSI is operation without any damp term.

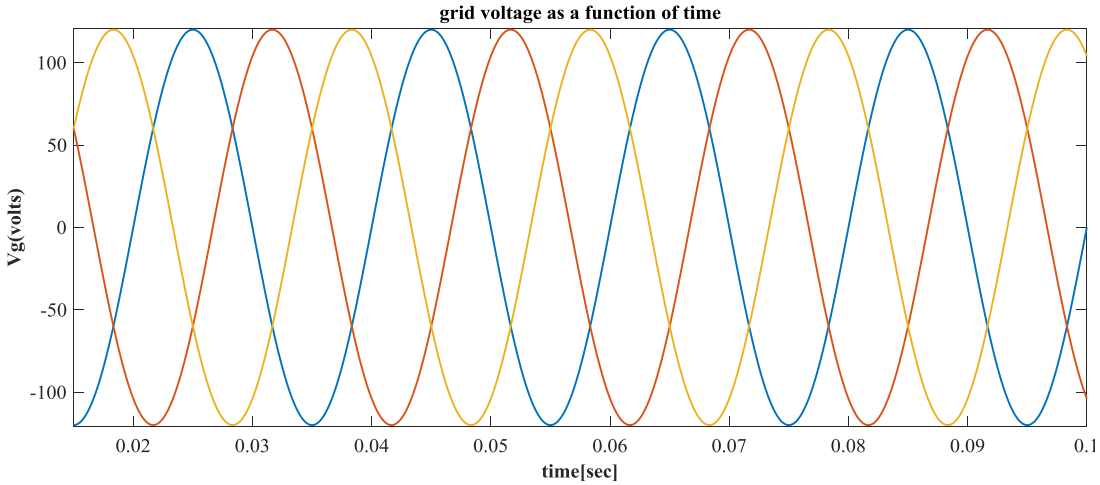

(a)

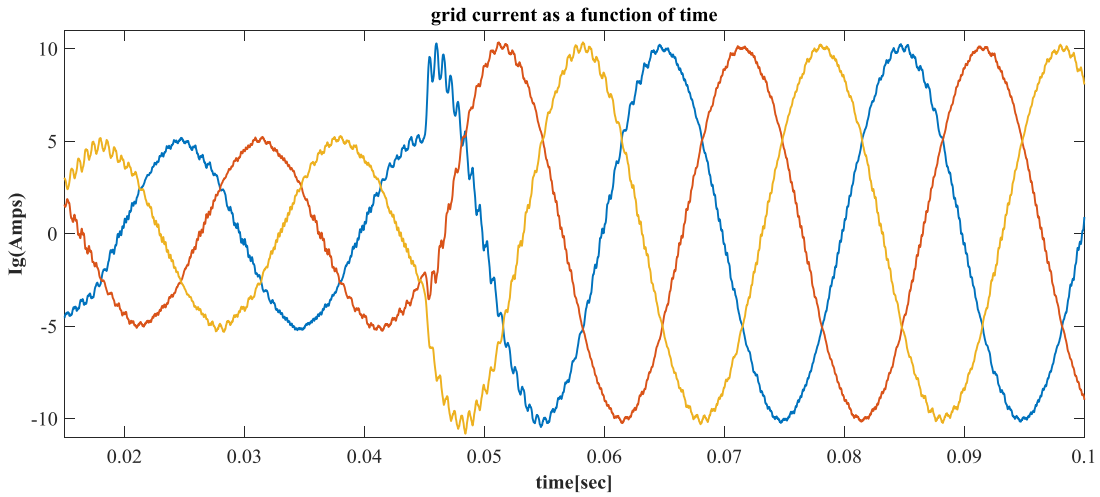

(b)

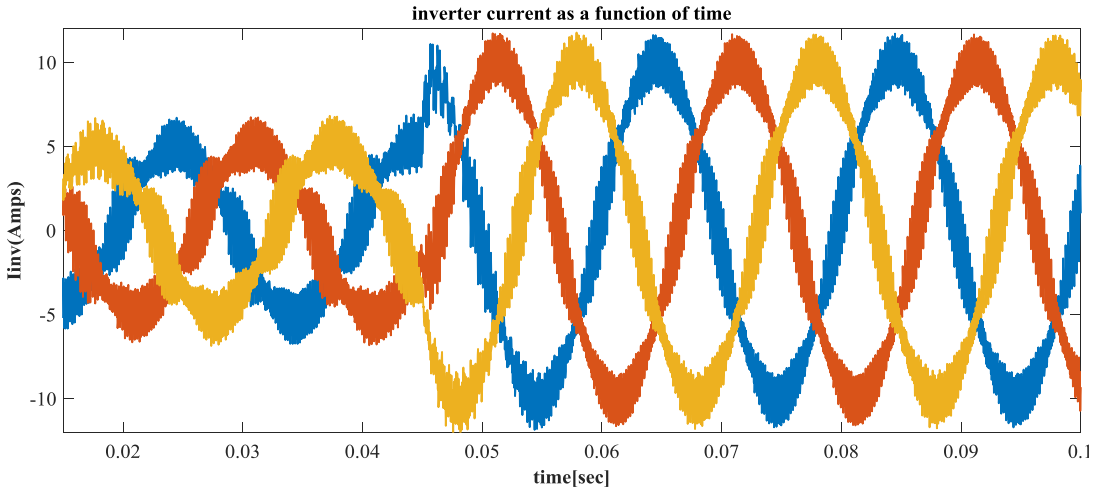

(c)

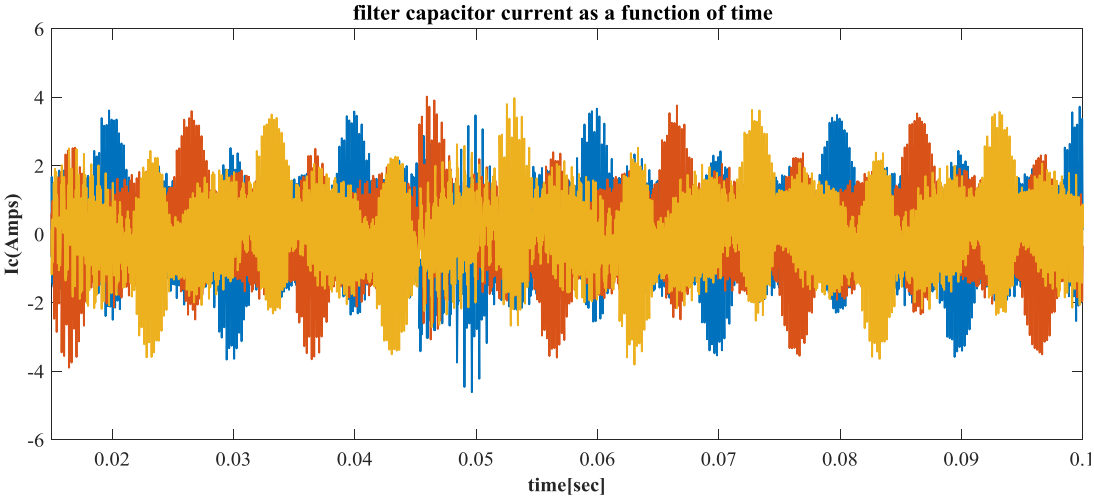

(d)

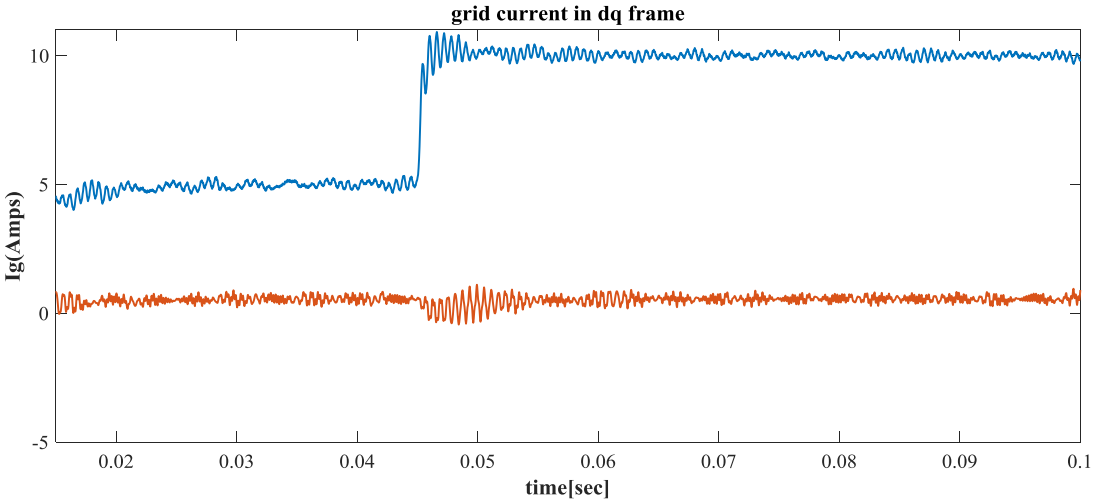

(e)

Figure 21: Simulated results using grid current feedback control (a) grid voltage (b) grid current (c) inverter current (d) filter capacitor current and (e) grid current in *dq* frame.

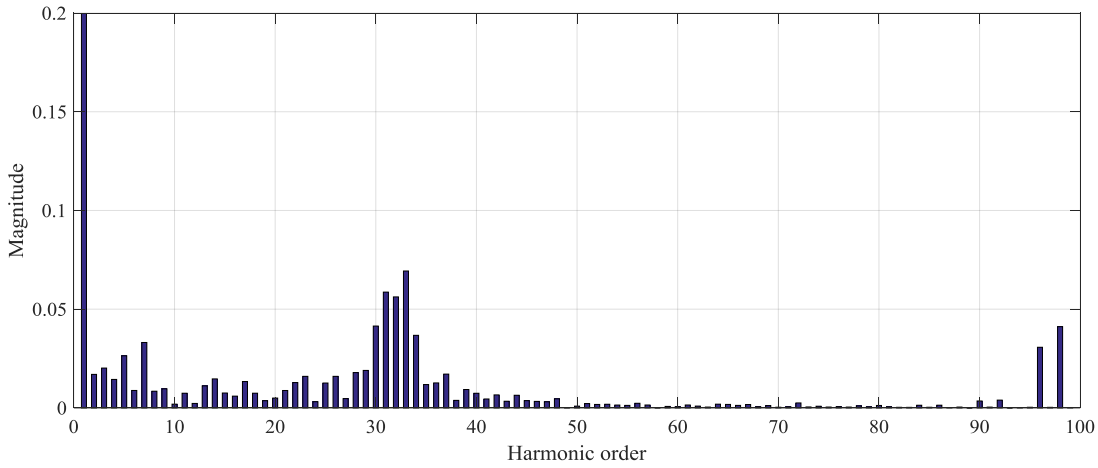

Figure 22: Harmonic spectrum of grid current using grid current feedback control

Chapter 5

CONCLUSION AND FUTURE WORK

5.1 Conclusion

The main goal here is to illustrate two different methods to properly damp the resonance of LCL-filter with current control for grid-connected three-phase VSI. Now it's verified that converter current control for feedback is the best because of its especial natural characteristic of LCL-filter. Optimum damping with a suitable control bandwidth was achieved in this thesis by using a proper design for the values of the grid and inverter inductors. When LCL-filter design is not satisfied due to some design constraints, another solution was presented to determine the capacitor current from the inverter current with the help of a notch filter and it's used for regulating the damping factor. To ensure the damping of the LCL-filter resonance, mathematical analysis was presented to determine the compensation gain. One of the advantages of this adopted control schemes is that one current sensor is required for feedback control to achieve the LCL filter damping resonance. Also the THD was measured to verify if the resonance was successfully suppressed. Simulations were executed using MATLAB SIMULINK and the results have been presented to prove the effectiveness of the adopted control strategy.

5.2 Future works

The following items are suggested as future work for the project:

- Stability analysis of grid-connected inverter with LCL filters applying a digital single-loop controller with inherent damping characteristic.

- Enhanced stability using grid current feedback control for LCL-filtered grid converters.
- Analysis of the passive damping losses in LCL-filter based grid converters
- A sliding-mode controller with multi-resonant sliding surface for single phase grid connected voltage source inverter with an LCL filter.
- A general discrete time model to evaluate active damping of grid converter with LCL filters.

REFERENCES

[1] Yi Tang, IEEE, Poh Chiang Loh, Member, IEEE, Peng Wang, IEEE, Fook Hoong Choo, and Feng Gao, Member, IEEE "Exploring Inherent Damping Characteristic of LCL-Filters for Three-Phase Grid-Connected Voltage Source Inverters" *IEEE Trans. Power Electron.,* Vol.27, NO. 3, MARCH 2012.

[2] G. Shen, D. Xu, L. Cao, and X. Zhu, "An improved control strategy for grid-connected voltage source inverters with an LCL-filter," *IEEE Trans. Power Electron.,* vol. 23, no. 4, pp. 1899–1906, Jul. 2008.

[3] M. Liserre, F. Blaabjerg, and S. Hansen, "Design and control of an LCLfilter-based three-phase active rectifier," *IEEE Trans. Ind. Appl.,* vol. 41, no. 5, pp. 1281–1291, Sep./Oct. 2005.

[4] D. G. Holmes, T. A. Lipo, B. P. McGrath, and W. Y. Kong, "Optimized design of stationary frame three-phase ac current regulators," *IEEE Trans. Power Electron.,* vol. 24, no. 11, pp. 2417–2426, Nov. 2009.

[5] F. Liu, Y. Zhou, S. X. Duan, J. J. Yin, B. Y. Liu, and F. R. Liu, "Parameter design of a two-current-loop controller used in a grid-connected inverter system with LCL-filter," *IEEE Trans. Ind. Electron.,* vol. 56, no. 11, pp. 4483–4491, Nov. 2009.

[6] E. Twining and D. G. Holmes, “Grid current regulation of a three-phase voltage source inverter with an LCL input filter,” *IEEE Trans. Power Electron.,* vol. 18, no. 1, pp. 373–380, Jan. 2003.

[7] Anugu Sarıtha, T. Abhiram, DR. K. Sumanth. “Space vector pulse width modulation for two level Inverter.*” International journal of professional engineering studies.* Volume VI /Issue 3 / MAY 2016.

[8] P.A. Dahono. “A method to damp oscillations on the input LC filter of current-type ac-dc pwm converters by using a virtual resistor.” *In Telecommunications Energy Conference,* 2003. INTELEC ’03. The 25th International, pages 757–761, 19-23 Oct. 2003.

[9] P. C. Loh and D. G. Holmes, “Analysis of multiloop control strategies for LC/CL/LCL-filtered voltage-source and current-source inverters,” *IEEE Trans. Ind. Appl.,* vol. 41, no. 2, pp. 644–654, Mar./Apr. 2005.

[10] P. A. Dahono, “A control method to damp oscillation in the input LC filter,” in Proc. *IEEE Power electron. Spec. Conf.,* 2002, vol. 4, pp. 1630–1635.

[11] T. Abeyasekera, C. M. Johnson, D. J. Atkinson, andM. Armstrong, “Suppression of line voltage related distortion in current controlled grid connected inverters,” *IEEE Trans. Power Electron.,* vol. 20, no. 6, pp. 1393–1401, Nov. 2005.

[12] W. Y. Kong, D. G. Holmes, and B. P. McGrath, “Improved stationary frame AC current regulation using feed forward compensation of the load EMF,” in *Proc. IEEE Appl. Power Electron. Conf.*, Washington, DC, CD record, 2009, pp. 145–151.

[13] D. N. Zmood and D. G. Holmes, “Stationary frame current regulation of PWM inverters with zero steady-state error,” *IEEE Trans. Power Electron.*, vol. 18, no. 3, pp. 814–822, May 2003.

[14] D. N. Zmood, D. G. Holmes, and G. H. Bode, “Frequency domain analysis of three-phase linear current regulators,” *IEEE Trans. Ind. Appl.*, vol. 37, no. 2, pp. 601–610, Mar. 2001.

[15] Zhang Guorong, Li Xun, Zhou Tonglu. “Parameter design of LCL filters for three-level converter based on space vector pulse width modulation.” *Transactions of the Chinese Society of Agricultural Engineering*, vol. 30, Number 19, 2014, pp. 214-221.

[16] M. Malinowski, M.P. Kazmierkowski, W. Szczygiel, and S. Bernet. “Simple sensorless active damping solution for three-phase pwm rectifier with LCL filter.” *Industrial Electronics Society*, 2005. IECON 2005. 31st Annual Conference of IEEE, page 5pp., 6-6 Nov. 2005.

[17] H.R. Karshenas, and H. Saghafi. “Basic criteria in designing LCL filters for grid connected converters.” *Industrial Electronics, IEEE International Symp., IEEE ISIE*, July 9-12, Montreal, Canada, vol. 3, pp. 1996-2000, 2006.

[18] Erickson, J., Robert, W., & Dragan, M. (2007). Fundamentals of power electronics. Springer Science & Business Media.

[19] Vodovozov, A., Valery. R., & Raik, J. (2006). *Power electronic converters*. Tallinn University of Technology Department of Electrical Drives and Power Electronics.

[20] Emre Kantar1, S. Nadir Usluer, and Ahmet M. Hava. "Design and Performance Analysis of a Grid Connected PWM-VSI System." in 8th *International Conference on Electrical and Electronics Engineering (ELECO)* 2013, pp.157- 161.

APPENDIX

Appendix A: Matlab/Simulink models

The simulation and implementation is built in Matlab/simulink are presented in this section.

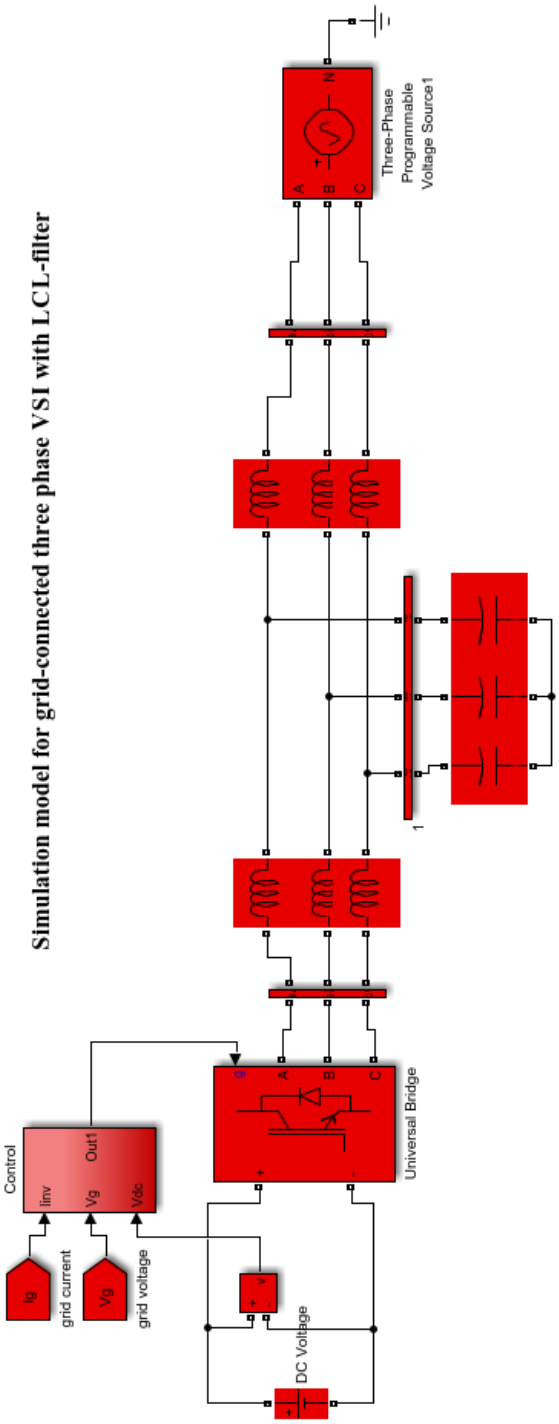

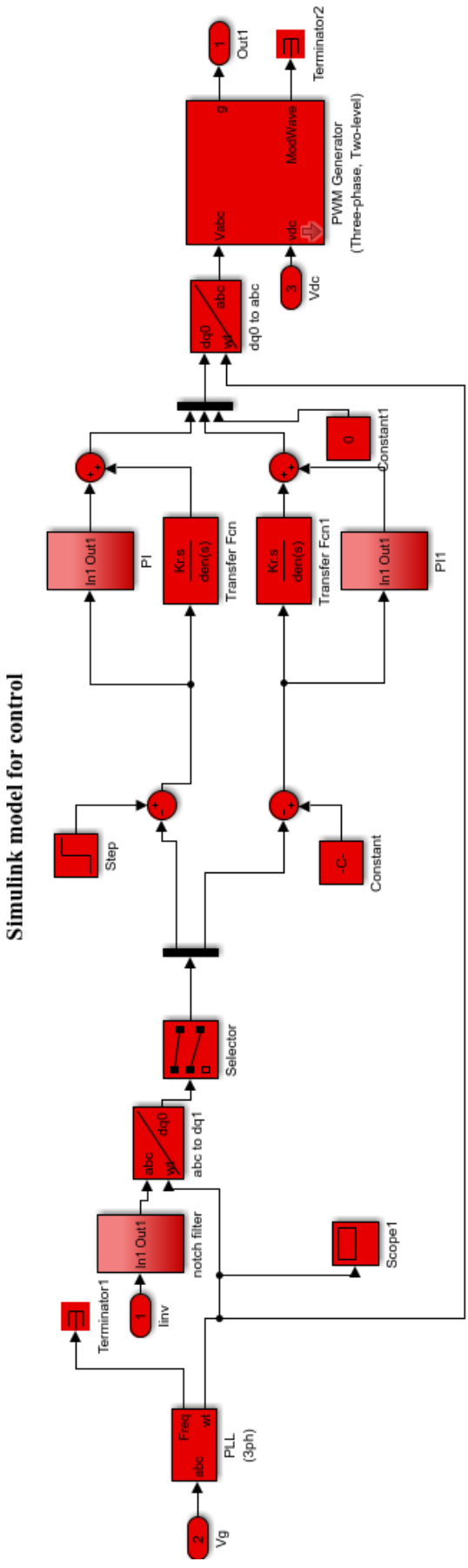
Simulink model for control
Vg
PLL (3ph)
Terminator1
linv
In1 Out1
notch filter
abc to dq1
Scope1
Selector
Step
PI
Transfer Fcn
Transfer Fcn1
PI1
Constant
Constant1
dq0 to abc
Vdc
PWM Generator (Three-phase, Two-level)
Out1
Terminator2